3632–3641 Nucleic Acids Research, 2002, Vol. 30 No. 16

Subcellular trafficking of antisense oligonucleotides and down-regulation of *bcl-2* gene expression in human melanoma cells using a fusogenic liposome delivery system

Qiang Hu[1,*], Marcel B. Bally[2] and Thomas D. Madden[1,3]

[1]Department of Pharmacology and Therapeutics, University of British Columbia, 2176 Health Sciences Mall, Vancouver, BC V6T 1Z3, Canada, [2]Division of Medical Oncology-Advanced Therapeutics, British Columbia Cancer Agency, 600 West 10th Avenue, Vancouver, BC V5Z 4E6, Canada and [3]Inex Pharmaceuticals Corporation, 8900 Glenlyon Parkway, Burnaby, BC V5J 5J8, Canada

Received March 19, 2002; Revised and Accepted June 5, 2002

ABSTRACT

Antisense oligonucleotides (ODN) targeted to specific genes have shown considerable potential as therapeutic agents. The polyanionic charges carried by these molecules, however, present a barrier to efficient cellular uptake and consequently their biological effects on gene regulation are compromised. To overcome this obstacle, a rationally designed carrier system is desirable for antisense delivery. This carrier should assist antisense ODN penetrate the cell membrane and, once inside the cell, then release the ODN and make them available for target binding. We have developed a carrier formulation employing programmable fusogenic vesicles (PFV) as the antisense delivery mediator. This study investigates the intracellular fate of PFV–ODN and bioavailability of antisense ODN to cells. The subcellular distribution of PFV and ODN was examined by monitoring the trafficking of FITC-labeled ODN and rhodamine/phosphatidylethanolamine (Rh-PE)-labeled PFV using confocal microscopy. Fluorescently tagged ODN were first co-localized with the liposomal carrier in the cytoplasm, presumably in endosome/lysosome compartments, shortly after incubation of PFV–ODN with HEK 293 and 518A2 cells. Between 24 and 48 h incubation, however, separation of FITC–ODN from the carrier and subsequent accumulation in the nucleus was observed. In contrast, the Rh-PE label was localized to the cell cytoplasm. The enhanced cellular uptake achieved using the PFV carrier, compared to incubation of free ODN with cells, and subsequent release of ODN from the carrier resulted in significant down-regulation of mRNA expression. Specifically, G3139, an antisense construct targeting the apoptotic antagonist gene *bcl-2*, was examined in the human melanoma cell line 518A2. Upon exposure to PFV-encapsulated G3139, cells displayed a time-dependent reduction in *bcl-2* message levels. The *bcl-2* mRNA level was reduced by 50% after 24 h treatment and by ~80% after 72 h when compared to cells treated with free G3139, empty PFV or PFV–G3622, a control ODN sequence. Our results establish that ODN can be released from PFV after intracellular uptake and can then migrate to the nucleus and selectively down-regulate target mRNA.

INTRODUCTION

Antisense therapy uses single-stranded synthetic oligodeoxynucleotides (ODN), unmodified or chemically modified, to regulate gene expression at the translational step. The potential specificity for target gene binding and consequent inhibition of gene products make antisense compounds an attractive new class of drugs for broad clinical applications (1–5). To achieve functional antisense activity, these specifically designed macromolecules need to be accumulated in the cell cytoplasm/nucleus and hybridize to corresponding target mRNA by Watson–Crick base pairing in a sequence-specific manner. The hybridization of ODN to mRNA will trigger endogenous RNase H activity, by far the most important inhibition mechanism of antisense activity, and initiate cleavage of the RNA strand. Alternatively, binding of exogenous DNA to mRNA can block downstream protein translation by disruption of ribosome assembly and inhibit target protein synthesis (6–9).

In the case of antisense therapy, the major limiting steps in its application include inefficient delivery of ODN to cells and poor bioavailability of ODN to intracellular targets (10,11). The polyanionic charges carried by these molecules present a barrier to efficient cellular uptake and consequently their biological activity on target gene regulation is significantly

*To whom correspondence should be addressed at present address: Inex Pharmaceuticals Corporation, 8900 Glenlyon Parkway, Burnaby, BC V5J 5J8, Canada. Tel: +1 604 456 6096; Fax: +1 604 419 3201: Email: qhu@inexpharm.com

compromised. To overcome this obstacle, a rationally designed carrier system is desirable for antisense delivery. This carrier should assist antisense ODN to penetrate the cell membrane and, once inside the cell, then release the antisense allowing target mRNA binding. We have developed a liposome system, programmable fusogenic vesicles (PFV), to mediate cellular delivery of encapsulated therapeutic agents (12,13). PFV consist of non-bilayer-forming lipids, which are stabilized in the liposome bilayer structure by exchangeable polyethyleneglycol (PEG)–lipid conjugates (14). Upon loss of these polymers from the liposome bilayer, which occurs through an exchange mechanism and can be designed to occur over periods from minutes to hours (15), the vesicles become unstable and fusogenic. Subsequently, fusion of the vesicles with the cell membrane could mediate the release of encapsulated agents into intracellular compartments. Recently, we employed PFV systems for antisense delivery and have developed a PFV–ODN formulation for efficient *in vitro* cellular uptake of antisense ODN (16). Our previous results demonstrate that cellular accumulation of antisense is significantly enhanced when antisense ODN are introduced to cells in an optimized PFV formulation, under conditions where the uptake of free antisense is negligible. Further investigation also indicates that the enhanced cellular uptake of antisense ODN results in enhanced biological activity. Interestingly, however, target mRNA down-regulation is delayed and the PFV–ODN formulation is less potent compared to cationic liposome formulations. This raises the question as to the fate of encapsulated antisense ODN once taken into cells. We do not know the subcellular location of PFV–ODN and the efficiency of oligonucleotide release from the PFV carrier and hence bioavailability to the target mRNA. To address these issues, we have carried out the current study to examine the subcellular distribution and bioavailability of antisense in PFV–ODN formulations.

In the present study, we have applied confocal microscopy to investigate subcellular trafficking of the lipid and antisense in PFV–ODN formulations. The pattern of intracellular fluorescent distribution of FITC-labeled antisense ODN is compared for different delivery systems. The bioavailability of antisense ODN is further evaluated with antisense G3139, an active antisense construct targeting the proto-oncogene *bcl-2*, in a human melanoma cell line. We have demonstrated that PFV-encapsulated antisense ODN is released from the carrier in a time-dependent manner. The freed antisense ODN can subsequently escape from the intracellular compartment in which it initially accumulates (endosome/lysosome) and migrate to the nucleus. Consistent with the observed rates of intracellular migration, the biological activity of the *bcl-2* antisense shows a time-dependent response. Based on our observations, a mechanism for PFV delivery of antisense ODN is proposed.

MATERIALS AND METHODS

Materials and chemicals

1,2-Dioleoyl-sn-glycero-3-phosphatidylethanolamine (DOPE) and 1,2-dioleoyl-sn-glycero-3-phosphatidylethanolamine-*N*-(lissamine rhodamine β sulfonyl) (Rh-PE) were purchased from Avanti Polar Lipids (Alabaster, AL). *N*,*N*-dioleyl-*N*,*N*-dimethyl ammonium chloride (DODAC) and monomethoxy polyethylene$_{2000}$glycol succinate ceramide-$C_{14:0}$ (PEG-C_{14}) were kindly provided by Inex Pharmaceuticals Corp. (Vancouver, BC). [^{3}H]cholesteryl hexadecyl ether ([^{3}H]CHE) was bought from NEN™ Life Science (Boston, MA). Cholesterol, DABCO, HEPES, paraformaldehyde, phenazine methosulfate (PMS), sodium thiocyanate (NaSCN), DEAE–Sepharose CL-6B and XTT were purchased from Sigma Chemical Co. (Oakville, ON). Dialysis tubing (SpectraPor 12 000–14 000 molecular weight cut-off) was obtained from Fisher Scientific (Ottawa, ON). Media and fetal calf serum for cell cultures, Trizol reagent, M-MLV reverse transcriptase, random hexamers and *Taq* DNA polymerase were originally obtained from Gibco BRL-Life Technologies (Burlington, ON). Antisense FITC–EGFR and mismatched control ODN were generous gifts from Inex Pharmaceuticals Corp. The antisense *bcl-2* (G3139) and reverse polarity control ODN (G3622) were originally synthesized by Genta Inc. (Lexington, MA).

Cell culture

HEK 293 human embryonic kidney cells (ATCC, Rockville, MD) and 518A2 human melanoma cells (British Columbia Cancer Agency) were maintained in Dulbecco's modified Eagle's medium (DMEM) supplemented with 10% heat-inactivated fetal calf serum at 37°C in 5% CO_2 and used at passages of 10–25. In all experiments, cells were seeded 16–18 h prior to treatment.

Oligonucleotides

Both the antisense and control sequences used in this study were fully phosphorothioated, linear, single-stranded ODN. The subcellular distribution of antisense ODN was examined using a 15mer, FITC 5′-labeled antisense construct targeting the stop codon of the human EGFR gene (5′-CCG TGG TCA TGC TCC-3′). The biological effect of the antisense was studied using a well designed 18mer antisense construct, G3139, with the sequence 5′-TCT CCC AGC GTG CGC CAT-3′. G3139 is complementary to the first six translation initiation codons of the open reading frame of the human *bcl-2* gene. The control ODN, G3622, for this antisense had the same sequence as that of G3139 but in the reverse polarity arrangement (5′-TAC CGC GTG CGA CCC TCT-3′). In addition, a 16mer control oligonucleotide with sequence 5′-T AAG CAT ACG GGG TGT-3′ was used in the cytotoxicity studies.

Preparation of PFV and encapsulation of ODN in PFV

Empty PFV and PFV-encapsulated ODN were prepared as described previously (16). Briefly, DOPE, cholesterol, DODAC and PEG-C_{14} were dissolved in 100% ethanol at molar ratios of 35:45:15:5. A trace amount of [^{3}H]CHE (~0.005 μCi/mg lipid) was included in the mixture as a lipid marker and 0.5 mol% Rh-PE was added when the liposomes were prepared for confocal microscopy studies. To prepare PFV-encapsulated ODN, the lipid mixture was added to a solution of antisense (1 mg/ml) in 200 mM NaCl buffered with 20 mM HEPES pH 7.4 (HBS), such that the final antisense:lipid ratio was 0.07:1 (w/w) and the final ethanol concentration was 30%. For the preparation of empty PFV, the lipid mixture was simply added to HBS. Vesicles were

subsequently extruded through 100 nm pore size polycarbonate filters to create unilamellar vesicles using an Extruder (Lipex Biomembranes, Vancouver, BC) (17). Ethanol was removed by dialyzing the vesicles against HBS overnight at room temperature. Free and externally bound antisense were removed by dialysis against 150 mM NaCl, 50 mM NaSCN, 20 mM HEPES, pH 7.4, for 5 h, followed by ion exchange chromatography (DEAE–Sepharose CL-6B). The final antisense:lipid ratio in loaded PFV was ~0.03–0.04:1 (w/w) and the encapsulation efficiency of the PFV was in the range 43–57%. The mean diameter of antisense-loaded PFV ranged from 100 to 120 nm as determined by quasi-elastic light scattering using a NICOMP Model 270 particle sizer. Vesicles for *in vitro* cell culture studies were sterilized by terminal filtration through a 0.2 μm HT Tuffryn membrane filter (Gelman Science, Ann Arbor, MI).

Preparation of cationic liposomes and liposome–ODN complexes

Cationic liposomes containing DOPE and DODAC were prepared using a standard procedure. Briefly, both lipids were dissolved in benzene:methanol (95:5 v/v) at a molar ratio of 50:50 and then lyophilized for a minimum of 5 h at a pressure of <60 mTorr using a Virtis lyophilizer equipped with a liquid N_2 trap. The dried lipid film was hydrated by vortexing in distilled H_2O to form multilamellar vesicles. Unilamellar vesicles were then sequentially prepared by extrusion through 100 nm pore size polycarbonate filters after freeze–thawing cycles (18).

Cationic liposome–ODN complexes were prepared by mixing preformed cationic liposomes with an equal volume of ODN in sterile distilled water and incubated at room temperature for 30 min before addition to the cells. The concentrations of total lipid and ODN in the complex preparation were adjusted according to the desired charge ratio. The final charge ratio of cationic lipids:ODN used in this study was 1.5:1.

Confocal microscopy analysis

Cells were plated in Lab-Tek chambered coverglasses at 1×10^4 cells/chamber in a volume of 1 ml. FITC-labeled antisense ODN, provided in the form of free, PFV-encapsulated or cationic liposome complex, were added to cells at a final antisense concentration of 0.5 μM. For free or PFV-encapsulated antisense treatment, cells were maintained in normal medium containing 10% fetal calf serum. For cationic liposome–ODN complex treatment, cells were incubated in serum-free medium for 4 h and, subsequently, the medium was replaced with one containing serum for longer time points. At 4, 24 or 48 h post-treatment, the cells were washed three times with PBS and fixed with 4% paraformaldehyde for 30 min at room temperature (19). After fixation, the cells were mounted in glycerol/PBS (1:1 v/v) containing 2.5% DABCO as an antifading agent and kept at 4°C for at least 1 h before confocal microscopy. The subcellular localizations of FITC-labeled antisense and Rh-PE-labeled PFV were assessed using a laser scanning confocal image system (Radiance 2000; Bio-Rad) equipped with a Zeiss 100 T-inverted microscope and a 63× oil immersion objective (NA 1.4). The laser was set to produce 488 (blue) and 543 nm (yellow) excitation wavelengths for fluorescein and rhodamine. Dual images were acquired sequentially with a Kalman filter (average of four images). The final projection image was processed using Scion Image software (Scion Corp., MD) and color photographs were obtained using Adobe Photoshop.

Measurement of cytotoxicity

The *in vitro* cellular toxicities of PFV and cationic liposomes were evaluated using the XTT tetrazolium salt assay (20). Briefly, cells were plated into 24-well plates at 1×10^4 (518A2) or 2×10^4 cells/well (HEK 293) in a volume of 0.4 ml. PFV–ODN or cationic liposome–ODN complexes were added to cells at incremental lipid concentrations. The experimental conditions were identical to those of the delivery and gene regulation studies. At 24 or 48 h post-exposure to liposomes, freshly prepared XTT solution containing 1% PMS was added to each well at 20% of the total volume and the plates were incubated at 37°C for 3 (518A2) or 4 h (HEK 293). At each time point, the well contents were removed to test tubes containing 1% Triton X-100 and absorbance was evaluated at 450 nm with a spectrophotometer. Cell viability was calculated based on a standard curve and expressed as a percentage of surviving cells as compared to control cell numbers.

Evaluation of *bcl-2* mRNA expression by RT–PCR

518A2 cells were cultured in 6-well plates at an initial density of 3×10^5 cells/well in a volume of 2 ml. Antisense ODN were added to the cells either as the free form or in the PFV–ODN formulation. Control cells were treated with the same volume of HBS. In addition, cells were also treated with empty PFV or PFV-encapsulated control ODN to monitor any potential non-specific effects. Cells were continuously exposed to each treatment up to RNA assay. At 24, 48 or 72 h post-treatment, the medium was removed and the cells were directly lysed in the well. Total RNA was extracted using Trizol reagent following the manufacturer's instructions.

The level of *bcl-2* mRNA expression was evaluated using semi-quantitative RT–PCR following a standard procedure (21). Briefly, first strand cDNA was synthesized from 2 μg total RNA using M-MLV reverse transcriptase and random hexamers in 50 mM Tris–HCl pH 8.3, 75 mM KCl, 10 mM DTT and 2 mM dNTPs. The reaction was allowed to proceed for 1 h at 37°C and stopped by incubation of the reaction mixture at 95°C for 5 min. Reverse transcription reaction products subsequently underwent PCR amplification for the detection of specific genes. Aliquots of RT reaction products were amplified separately for *bcl-2* and β-actin by PCR in 20 mM Tris–HCl pH 8.4, 50 mM KCl, 1.5 mM $MgCl_2$, 0.8 mM dNTPs, 0.25 μM each of the gene-specific primers and 1.5 U *Taq* DNA polymerase. The primer pair for *bcl-2* was 5′-atggcgcacgctgggagaac-3′/5′-gcggtagcggcgggagaagt-3′ (327 bp amplified product) and for β-actin was 5′-tgatccacatctgctg-gaaggtgg-3′/5′-ggacctgactgactacctcatgaa-3′ (524 bp amplified product). DNA amplification was performed using a Perkin-Elmer DNA thermocycler under the following conditions: 30 s at 94°C, followed by 1.5 min at 65°C for 20 or 35 cycles. Appropriate cycle numbers were determined experimentally for each gene in the cell line tested to yield exponential amplification. Amplified products were electrophoresed in a 1.5% (w/v) agarose gel stained by ethidium bromide. Levels of relative band intensity, corrected on the basis of β-actin

level, were quantitated using a digital camera (Eagle Eye™ II; Stratagene) coupled with ImageQuant software (Molecular Dynamic, CA). The final values of *bcl-2* mRNA abundance were expressed as a percentage of the untreated control cells.

Statistical analysis

Data from gene regulation studies were evaluated by one-way ANOVA using SigmaStat software. Differences among treatment groups were further evaluated with the Student–Newman–Keuls test. A statistically significant difference was reported for $P < 0.05$.

RESULTS

Cytoplasmic co-localization of antisense ODN and PFV at an early incubation time

In previous investigations, we demonstrated enhanced *in vitro* cellular uptake of antisense by PFV delivery. The present studies were therefore aimed at characterizing the intracellular distribution and trafficking of both the oligonucleotide and PFV carrier. This was investigated in two cell lines: HEK 293 and 518A2 cells. Free antisense, cationic liposome/antisense complexes or PFV-encapsulated antisense ODN were added to cells at a final concentration of 0.5 μM. Subcellular trafficking of antisense ODN and PFV was examined by monitoring the distribution of FITC-labeled ODN and Rh-PE-labeled PFV using confocal microscopy. As shown in Figure 1, antisense accumulation and distribution within cells was highly dependent on carrier delivery. When antisense ODN were incubated with cells for 4 h as the free agent, cellular uptake was generally very poor, although 518A2 cells showed a slightly higher fluorescence intensity than HEK 293 cells (Fig. 1A and D). In contrast, cells exhibited massive internalization of both carrier and antisense ODN when the antisense ODN were delivered by PFV (Fig. 1B and E). At 4 h, a substantial majority of the antisense ODN was co-localized with PFV in the cell cytoplasm as punctate fluorescence. This co-localization of the green FITC fluorophore and red rhodamine fluorophore gives rise to the observed yellow color. In addition, some red fluorescence, mainly distributed around the cell plasma membranes, was also observed. However, its intensity was very weak compared to the co-localized fluorescent emission. Similarly, relatively weak green fluorescent spots were seen scattered in the cytoplasmic compartment in some cells. This may represent a low level of free antisense even at this 4 h time point. In both cell lines, the accumulation of co-localized carrier and ODN was predominantly in perinuclear regions. This pattern of intracellular distribution was distinct from that seen when ODN was delivered in the form of cationic liposome–ODN complexes. As shown in Figure 1C and F, using cationic liposome complexes, most of the antisense ODN were rapidly accumulated in the cell nucleus and only a small percentage was still present in the cytoplasm, particularly the perinuclear region, at 4 h. This pattern is consistent with previous observations in the literature and demonstrates that cationic liposomes are an effective mediator for ODN delivery (22–25). The nuclear distribution of antisense ODN was not homogeneous. As shown by the intensity of fluorescence, oligonucleotides were largely absent from the nucleolus

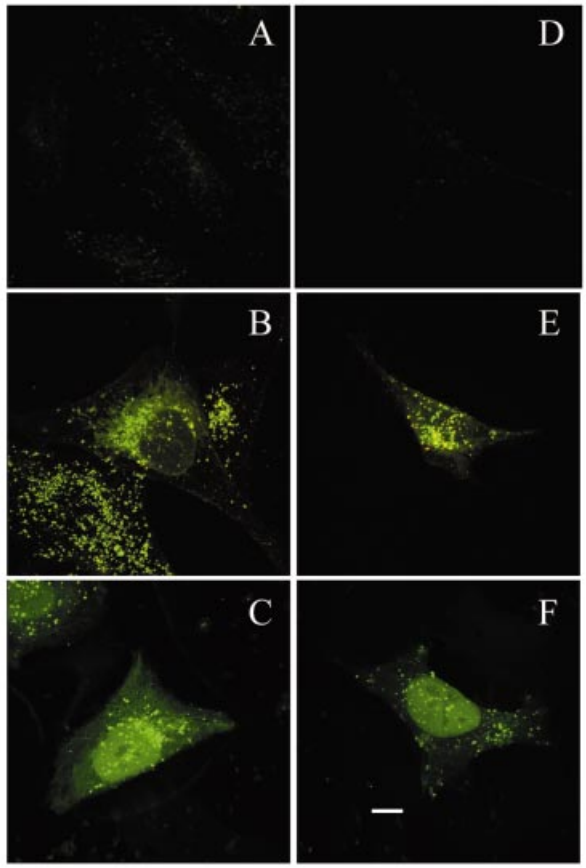

Figure 1. Confocal microscope projection image of cellular distribution of antisense ODN in 518A2 (**A**–**C**) and HEK 293 cells (**D**–**F**). Cells were exposed to free antisense ODN (A and D), PFV-encapsulated antisense ODN (B and E) or cationic liposome–antisense ODN complexes (C and F) for 4 h. Scale bar 10 μm.

compartment. The internalization of PFV-mediated antisense ODN and subsequent accumulation around the perinuclear region were further characterized by *z*-position laser scanning imaging (Fig. 2). These optical sections clearly indicated that the intensive fluorescence displayed in Figure 1E was predominantly from internal FITC–ODN and did not result from plasma membrane binding.

Time-dependent release of antisense ODN from PFV

To initiate an antisense effect, the ODN needs to be released from the carrier and hence available for target message binding. Obviously, after 4 h incubation the PFV carrier had efficiently mediated antisense accumulation within a cytoplasmic compartment. The next question was whether the accumulated antisense ODN could be released from the PFV carrier, exit the cytoplasmic compartment and access the nucleus. This was explored by following the intracellular distribution of PFV–ODN for 24–48 h. After 24 h incubation, cells exhibited signs of free FITC–ODN (Fig. 3). This was more clearly displayed in 518A2 cells (Fig. 3B). Comparing the Rh-PE distribution (red fluorescence) with the FITC–ODN distribution (green fluorescence) in the same cell (Fig. 3B-1 and B-2), it can be seen that the PFV are widely distributed in the cell cytoplasm while the FITC–ODN are mainly

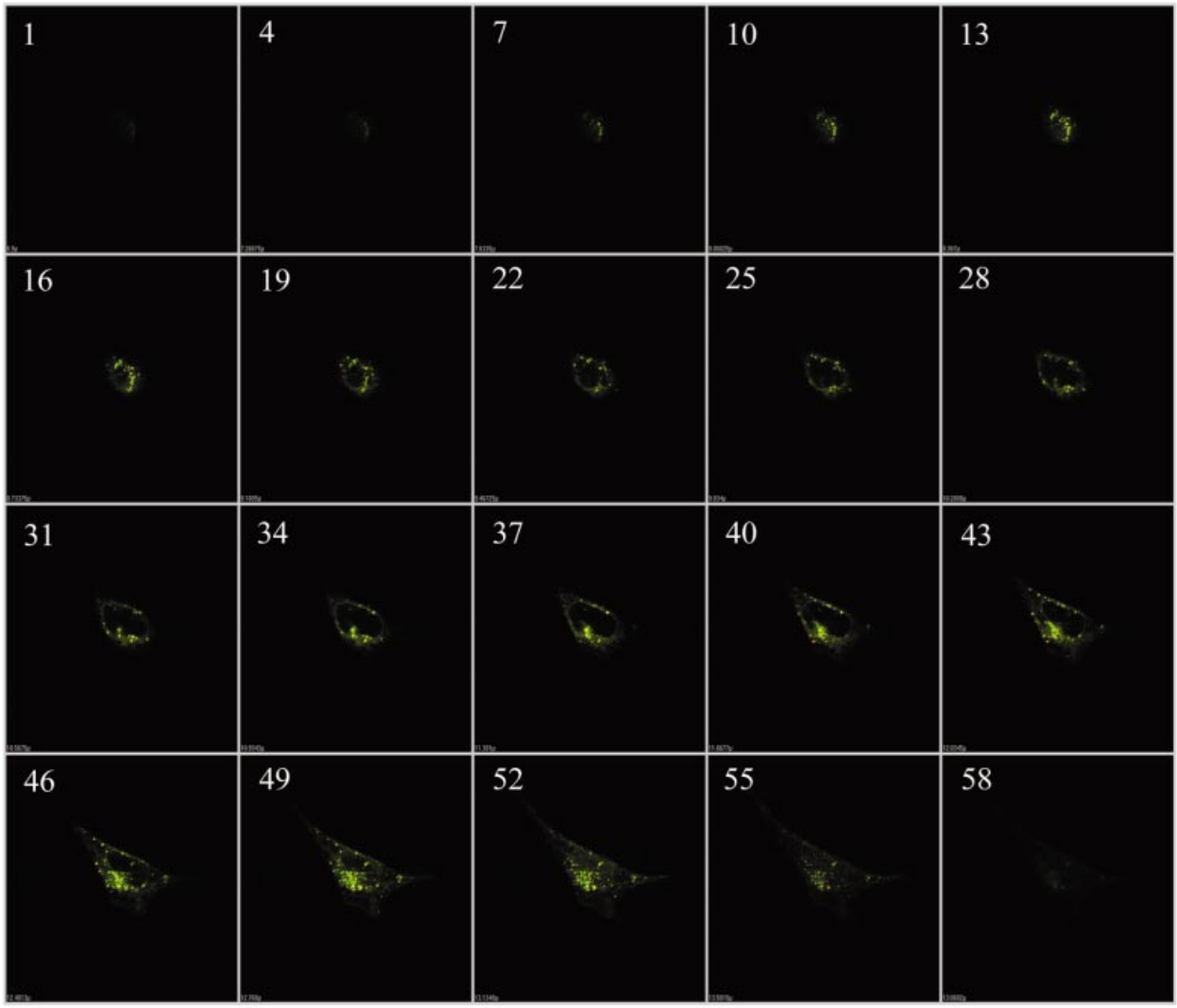

Figure 2. Representative optical sections displaying internalization and perinuclear accumulation of antisense ODN by PFV delivery. HEK 293 cells were incubated with PFV–ODN for 4 h and analyzed by confocal laser scanning. The optical sections (total 59) were scanned incrementally along the *z*-axis of the cell at a space distance of 0.15 μm. Section numbers on the *z*-axis are given in the upper left corner.

accumulated around, or within, the nucleus. This separation of ODN from the PFV carrier and subsequent migration into the nucleus was further evident after 48 h incubation with PFV–ODN (Fig. 4). As shown in Figure 4, intensive nuclear fluorescence (FITC) is seen for PFV–ODN delivery (Fig. 4B and D). Although one 518A2 cell in Figure 4B shows evidence of apoptosis, the other cells still possessed intact cell membranes, which is strong evidence of their viability. In these viable cells, FITC–ODN was distributed in both the cytoplasm and nucleus while the Rh-PE label remained exclusively in the cytoplasm (Fig. 4B-1 and B-2). A similar pattern was observed in HEK 293 cells (Fig. 4D), but with a much lower level of fluorescence intensity. The reason why HEK 293 cells show less nuclear fluorescence is not clear. As displayed after antisense delivery using cationic liposomes, once in the cell nucleus, FITC–ODN distribution was not homogeneous and the oligonucleotide appeared to be excluded from the nucleoli.

Effect of PFV–ODN on cell cytotoxicity

It has been well recognized that cationic lipids are very toxic to cells. Since PFV contain the cationic lipid DODAC, we conducted experiments to investigate the potential toxicity of PFV–ODN on 518A2 and HEK 293 cells. Cells were treated with PFV–control ODN or cationic liposome–control ODN complexes at various concentrations for 24 or 48 h. At these time points, cells were processed and cytotoxicity was assessed by XTT assay. As shown in Figure 5, both 518A2 and HEK 293 cells showed severe cytotoxic effects when treated with cationic liposome–ODN complexes. This toxicity was seen even at a lipid concentration as low as 50 μM. In both cell lines, less than 10% of cells were viable after 24 h incubation, and after 48 h few viable cells were seen. This result was consistent with our observations of cationic liposome–OND complex-treated cells under confocal microscopy. In contrast to cationic liposome–ODN complexes, the

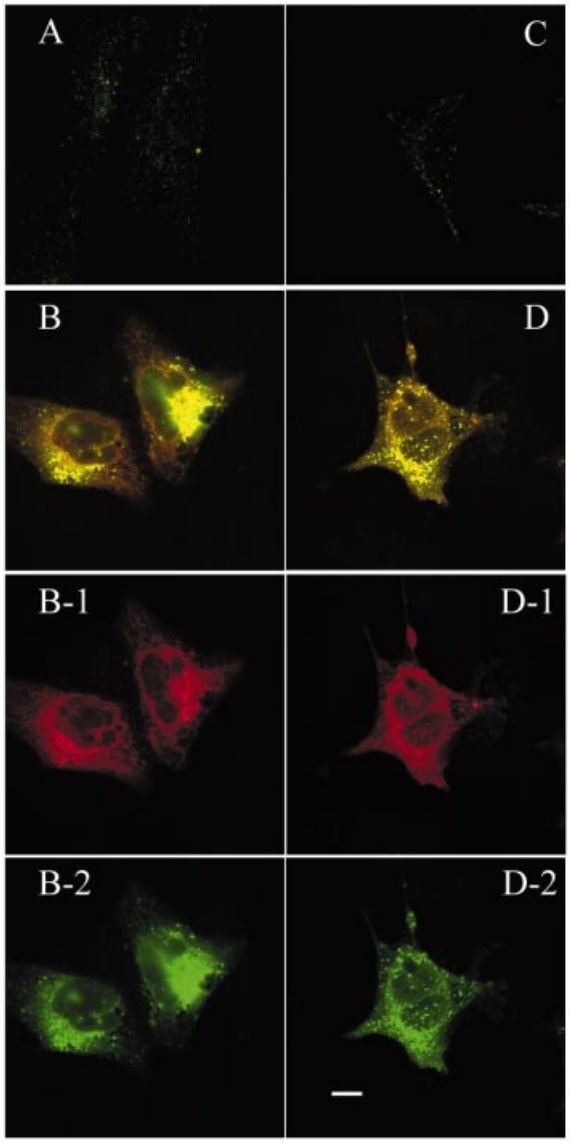

Figure 3. Confocal microscopy projection image of cellular distribution of antisense ODN in 518A2 (**A** and **B**) and HEK 293 cells (**C** and **D**) after 24 h exposure to free antisense (A and C) or PFV-encapsulated antisense (B and D). Rh-PE label is displayed as a red fluorescent image (**B-1** and **D-1**) and antisense ODN is displayed as a green fluorescent image (**B-2** and **D-2**). Scale bar 10 μm.

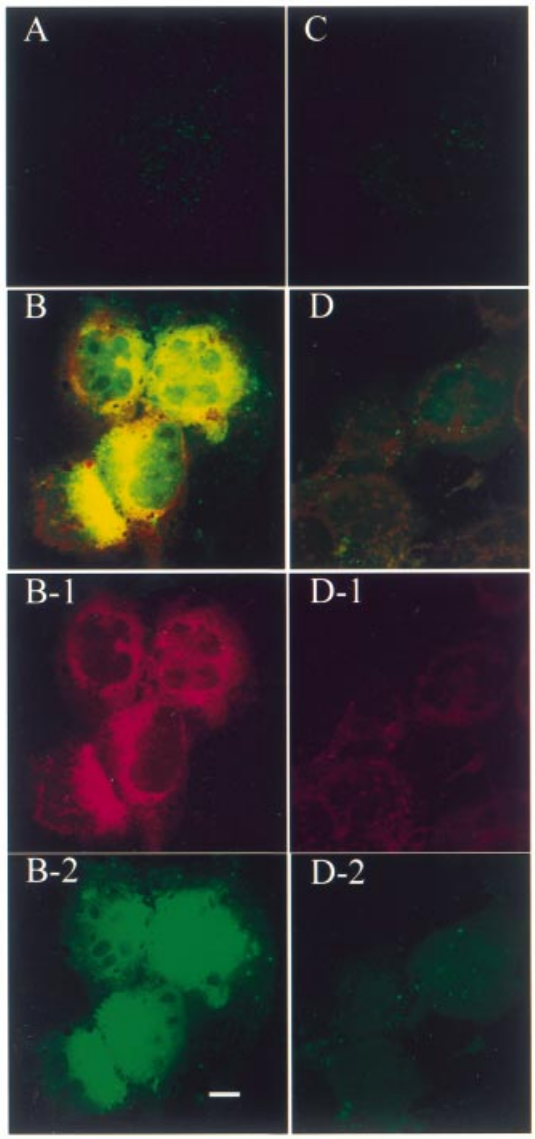

Figure 4. Confocal microscopy projection image of cellular distribution of antisense ODN in 518A2 (**A** and **B**) and HEK 293 cells (**C** and **D**) after 48 h exposure to free antisense (A and C) or PFV-encapsulated antisense (B and D). Rh-PE label is displayed as a red fluorescent image (**B-1** and **D-1**) and antisense ODN is displayed as a green fluorescent image (**B-2** and **D-2**). Scale bar 10 μm.

PFV–ODN formulation was less cytotoxic to both cell lines tested. As seen in Figure 5, after 24 h incubation with PFV–ODN, ~80% of cells were viable at low lipid concentrations. As the lipid concentration was increased, a gradual reduction in cell viability was observed. However, even at relatively high lipid concentrations (600 μM) >60% cell viability was seen. Over longer exposure periods a further reduction in cell viability was exhibited when cells were incubated with PFV–ODN. At the highest tested lipid concentration (600 μM), cell viability dropped to 30–40% at 48 h.

Time-dependent biological activity of PFV-encapsulated antisense ODN

The time-dependent release of antisense ODN from PFV and subsequent migration to the nucleus might be anticipated to result in a delay in down-regulation of the target mRNA. We therefore conducted a study on the human melanoma cell line 518A2 using G3139, an 18mer antisense ODN targeting the human *bcl-2* gene. Previous studies have shown that this antisense construct, delivered using cationic liposomes, is effective in down-regulation of its target message and this can result in a profound reduction in protein expression levels (26). In a previous study, however, we only observed a mild,

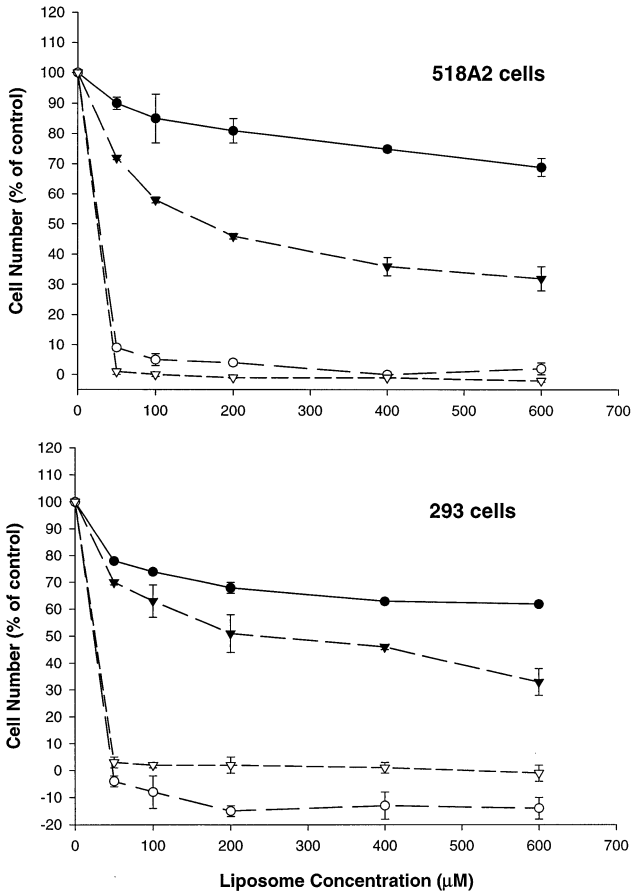

Figure 5. Effect of time and lipid concentration on cellular viability. 518A2 and HEK 293 cells were incubated with PFV–ODN (closed circles and closed triangles) or cationic liposome–ODN complexes (open circles and open triangles) at various lipid concentrations. Cells were assessed for cytotoxicity using the XTT assay after 24 (closed and open circles) or 48 h incubation (closed and open triangles) as described in Materials and Methods. Cell viability was expressed as a percentage of surviving cells as compared to untreated control cells. Values (means ± SD) were obtained from two or three experiments and each experiment was done in triplicate.

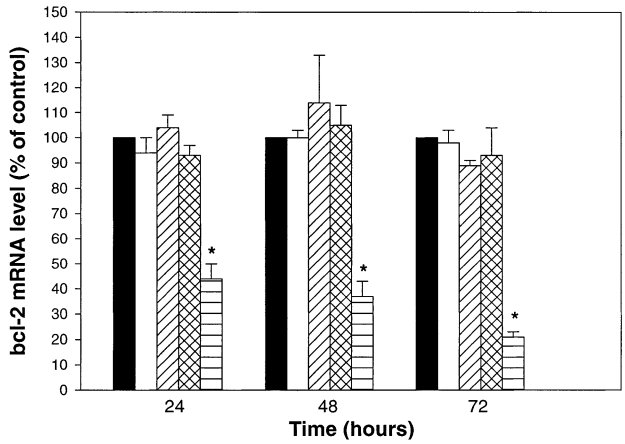

Figure 6. Expression of *bcl-2* mRNA in 518A2 cells upon exposure to HBS (shaded bar), free antisense (open), empty PFV (diagonal hatched), PFV–control ODN (G3622) (cross-hatched) or PFV–antisense ODN (G3139) (horizontal) at a final antisense concentration of 3.0 μM. The abundance of *bcl-2* mRNA was evaluated by RT–PCR. Values were presented as means ± SEM (n = 3). *, Significant difference between PFV–antisense ODN group and the rest of the treatment groups ($P < 0.05$).

but consistent, reduction in mRNA expression when cells were treated with PFV–ODN at 1.0 μM for 48 h (16). We speculated, based on our current observations, that this low activity was possibly due to the antisense ODN, delivered using PFV, not being completely available for subcellular target binding, or the concentration of slowly released antisense ODN being below a threshold level required to achieve significant activity. In the present study, therefore, we examined higher concentration of PFV–ODN over longer exposure periods. Cells (518A2) were treated with free antisense, empty PFV, PFV-encapsulated control ODN G3622 or PFV-encapsulated antisense ODN G3139 for 24, 48 or 72 h at an antisense concentration of 3.0 μM (or equivalent PFV concentration). At each time point, cells were harvested and processed for mRNA expression using RT–PCR. The data are shown in Figure 6. As can be seen, an antisense-specific down-regulation of *bcl-2* mRNA was clearly observed when cells were exposed to PFV-encapsulated antisense. At the tested antisense concentration the mRNA level was reduced by ~50% after 24 h incubation, while no down-regulation effect was observed for cells treated with free antisense, empty PFV or PFV-encapsulated control ODN. After 48 h incubation, PFV–antisense ODN-treated cells showed a further reduction of mRNA level, by ~65% compared to the control cells. Finally, at 72 h the mRNA expression in these cells was reduced by 80% when compared with cells treated with free antisense, empty PFV or PFV–control ODN. It has been observed that cytotoxicity effects alone can result in target gene inhibition, which has nothing to do with the antisense ODN (27). Since the *bcl-2* gene is involved in the cellular apoptosis pathway, there is a possibility that its expression will be affected by cell viability. Based on this concern, we used empty PFV as a control to monitor any potential non-specific effect on *bcl-2* mRNA levels as a consequence of cytotoxicity. Our results show that at all tested time points the cells did not show a significant reduction in mRNA level when treated with empty PFV, which were more toxic to cells than equivalent concentrations of PFV–ODN (data not shown). Similarly, when cells were exposed to the PFV-encapsulated control ODN, which has the same base sequence as G3139 but in the reverse polarity, while preserving the CpG motifs, mRNA reduction was also not evident. We therefore conclude that the observed reduction in *bcl-2* mRNA level was due to an antisense ODN-specific effect.

DISCUSSION

Ever since the concept of using oligonucleotides to regulate gene expression was proposed (28), accumulated studies have demonstrated that these synthetic exogenous antisense ODN could play a role in disease treatment by reducing target mRNA and protein product levels (29–32). This effect will only be achieved, however, after intracellular uptake of these polyanionic molecules and migration to the nucleus. It has been suggested that internalization of free antisense ODN is mediated by cell surface-bound protein followed by endocytosis; however, it is recognized that this process is

inefficient and highly variable between cell types (33–35). This limitation can be addressed *in vitro* through the use of cationic liposomes. By forming a complex structure with antisense ODN, these cationic liposomes can not only enhance the non-specific cellular uptake of antisense ODN through charge–charge interactions, but also facilitate antisense escape from the endosomal compartment and hence allow target mRNA binding (24,25). However, the use of cationic liposome complexes for antisense delivery is handicapped by their toxicity and the fact that they are metastable and hence unsuitable for systemic application. Recently, we have developed a PFV–ODN formulation as a potential carrier system for systemic antisense delivery. These PFV systems are designed to be much more stable than cationic liposomes and hence suitable for systemic use. Further, the oligonucleotide is largely encapsulated within the carrier, rather than being complexed to the exterior surface. PFV contain a cationic lipid, DODAC, that is initially shielded by the steric barrier afforded by the PEG-ceramide component. However, after PEG-ceramide is lost from the vesicle surface, through an exchange mediated process (36), the exposed cationic charge will promote association with cell membranes leading to endocytosis. Loss of PEG-ceramide also results in destabilization of the vesicle bilayer, potentially triggering fusion with adjacent membranes. The rate of loss of PEG-ceramide can be controlled by the length of the acyl chains 'anchoring' this component in the bilayer (15). A previous study has demonstrated that encapsulation of antisense ODN in properly designed PFV can significantly enhance their cellular uptake compared to free antisense (16). As a result, increased biological activity is subsequently observed. However, we know little about the intracellular distribution and trafficking of both lipid and antisense ODN in the PFV–ODN formulation once they are taken into cells. The efficiency of antisense release from the carrier, and hence availability for target mRNA hybridization, is clearly critical with respect to biological activity.

In the present study, we confirm that cellular uptake of free antisense is very inefficient. The low levels of fluorescence seen indicate that the free antisense is predominantly located in endosomes/lysosomes, consistent with an endocytic uptake mechanism. Further, our observations suggest that endosomal free antisense is released to the cytoplasm only slowly. On incubation of PFV–ODN with cells, both lipid and antisense ODN are quickly accumulated in the perinuclear region of the cell cytoplasm. Since this region is known to be predominantly occupied by the endosome and lysosome compartments, we speculate that the initial uptake of PFV–ODN into cells is largely assisted by endocytosis. Within this endosomal compartment only slow release of oligonucleotide from the lipid carrier, and subsequent migration to the nucleus, is seen. This is in contrast to the rapid nuclear localization of antisense seen on incubation of cationic liposome–ODN complexes with cells (22–24). In the case of cationic liposome–ODN complexes, it has been suggested that following uptake into the endosome, the complex initiates destabilization of the endosomal membrane resulting in a flip-flop of anionic lipids, which subsequently form ion pairs with the cationic lipid and release the ODN from the complex (37,38). Free antisense ODN are then able to migrate to the nucleus, although the mechanism for this migration is still not very well understood. The difference in the rate of intracellular trafficking we see between cationic liposome–ODN complexes and PFV–ODN is in agreement with the expected greater stability of the PFV–ODN systems. Our results confirm that release of PFV-encapsulated antisense ODN and accumulation in the cell nucleus does occur for PFV–ODN in a time-dependent manner. Over 48 h, for example, substantial nuclear localization of ODN is achieved, while fluorescent lipids are exclusively associated with cytoplasmic compartments. That the observed nuclear fluorescence represents FITC-labeled ODN rather than a degradation product such as FITC is supported by previous publications. Fisher and co-workers observed that if FITC was injected into cells, it rapidly diffused throughout the entire cellular compartment without a specific pattern or boundary limitation. Furthermore, the metabolites of degraded ODN were exported out of the nucleus more quickly than intact ODN (39). Based on their observations, we conclude that the subcellular fluorescence displayed in cells results from intact FITC–ODN.

Considering the biophysical properties of PFV systems and the pattern of fluorescent distribution, we propose the following model to explain the time-dependent ODN cellular uptake and endosomal release. PFV systems contain small amounts of PEG–lipid for the purpose of bilayer stabilization and charge shielding. Based on the fluorescence pattern observed at early time points, it seems clear that PFV–ODN have been taken up by endocytosis. This implies that sufficient PEG–lipid has been lost from the external bilayer to expose some cationic charge and allow absorption to the cell surface, but insufficient PEG–lipid has been lost to trigger vesicle–cell fusion. After endocytosis, the remaining PEG–lipid will continue the exchange process, which will eventually trigger vesicle destabilization and vesicle–endosome fusion. Fusion with the endosomal membranes will then initiate a series of cellular events similar to those proposed for the cationic liposome–ODN complex model, eventually leading to release of antisense ODN from the PFV and, subsequently, the endosomal compartments. In this model, we suggest that fusion with the endosomal membrane is the rate-limiting step for efficient release of antisense ODN. This model predicts an important role for the fusogenic lipid component, DOPE, in PFV–ODN. Indeed, previous studies conducted in our laboratory have shown that if DOPE is replaced by the non-fusogenic lipid DOPC in the PFV system, release of encapsulated agents into the cytoplasm and nucleus is significantly reduced (40). Further, this earlier work demonstrated that with conventional liposomes there is no cytoplasmic release of an encapsulated agent even though these liposomes can be taken up by endocytosis (41). Even with cationic liposome–ODN complexes, if DOPE is replaced by DOPC, no nuclear accumulation of ODN will be observed and both lipid and ODN are trapped in the endosomal compartments (42). The presence of fusogenic DOPE in the PFV formulation is a key factor to trigger endosomal membrane destabilization, which may initiate disruption of the membrane asymmetry (43). The proposed model is further supported indirectly by the results from cytotoxicity studies. We have observed that the potency of toxicity to cells among the different formulations is in the order cationic liposome > empty PFV > PFV–ODN. While for PFV–ODN the toxic effect on cells increases with extended incubation time. It is believed that the toxic effect is mainly

due to the cationic lipid component included in the formulation. Therefore, a reduced and delayed onset of this effect could be an indication of gradual exposure and bioavailability of these lipids for cellular interaction. For PFV–ODN this implies a gradual release of the antisense ODN.

The time-dependent release of antisense ODN from entrapped endosome/lysosome compartments is further supported by subsequent time-dependent antisense-specific activity. This was tested with antisense *bcl-2*, a widely accepted active antisense construct. These data are not only consistent with the subcellular trafficking observations, but also provide support for generally accepted antisense mechanisms. First, it supports the general belief that antisense ODN activity is concentration dependent (44). Second, it suggests that although down-regulation can occur in the cytoplasm, the most efficient antisense effect happens in the cell nucleus, which implies the involvement of RNase H activity (45).

In conclusion, our data clearly demonstrate that PFV systems not only enhance cellular uptake of antisense ODN, but also facilitate antisense ODN escape from subcellular compartments to the cytoplasm and nuclear compartments. This property is clearly important to achieve maximum therapeutic activity. Future studies will need to evaluate such delivery systems following systemic application. The proposed endosomal release mechanism of PFV–ODN formulations described in this study has general applicability to other similar non-bilayer lipid-containing liposome systems and deserves further *in vitro* investigation.

ACKNOWLEDGEMENTS

We gratefully acknowledge Dr Jeff Hewitt for his help in PCR primer design, Inex Pharmaceutical Co. for providing some facilities and two anonymous referees for their valuable comments and suggestions. This work was supported by a grant from the National Cancer Institute of Canada through funds provided by the Canadian Cancer Society (T.D.M. and M.B.B.).

REFERENCES

1. Hélène,C. and Toulmé,J.J. (1990) Specific regulation of gene expression by antisense, sense and antigen nucleic acids. *Biochim. Biophys. Acta*, **1049**, 99–125.
2. Crooke,S.T. (1992) Therapeutic applications of oligonucleotides. *Annu. Rev. Pharmacol. Toxicol.*, **32**, 329–376.
3. Jansen,B., Wacheck,V., Heere-Ress,E., Schlagbauer-Wadl,H., Hoeller,C., Lucas,T., Hoermann,M., Hollenstein,U., Wolff,K. and Pehamberger,H. (2000) Chemosensitisation of malignant melanoma by BCL2 antisense therapy. *Lancet*, **356**, 1728–1733.
4. Khuri,F.R. and Kurie,J.M. (2000) Antisense approaches enter the clinic. *Clin. Cancer Res.*, **6**, 1607–1610.
5. Tamm,I., Dörken,B. and Hartmann,G. (2001) Antisense therapy in oncology: new hope for an old idea? *Lancet*, **358**, 489–497.
6. Walder,R.Y. and Walder,J.A. (1988) Role of RNase H in hybrid-arrested translation by antisense oligonucleotides. *Proc. Natl Acad. Sci. USA*, **85**, 5011–5015.
7. Lavrovsky,Y., Chen,S. and Roy,A.K. (1997) Therapeutic potential and mechanism of action of oligonucleotides and ribozymes. *Biochem. Mol. Med.*, **62**, 11–22.
8. Baker,B.E. and Monia,B.P. (1999) Novel mechanisms for antisense-mediated regulation of gene expression. *Biochim. Biophys. Acta*, **1489**, 3–18.
9. Crooke,S.T. (1999) Molecular mechanisms of action of antisense drugs. *Biochim. Biophys. Acta*, **1489**, 31–44.
10. Akhtar,S. and Juliano,R.L. (1992) Cellular uptake and intracellular fate of antisense oligonucleotides. *Trends Cell Biol.*, **2**, 139–144.
11. Clark,R.E. (1995) Poor cellular uptake of antisense oligodeoxynucleotides: an obstacle to their use in chronic myeloid leukaemia. *Leuk. Lymphoma*, **19**, 189–195.
12. Holland,J.W., Hui,C., Cullis,P.R. and Madden,T.D. (1996) Poly(ethylene glycol)-lipid conjugates regulate the calcium-induced fusion of liposomes composed of phosphatidylethanolamine and phosphatidylserine. *Biochemistry*, **35**, 2618–2624.
13. Adakha-Hutcheon,G., Bally,M.B., Shew,C.R. and Madden,T.D. (1999) Controlled destabilization of a liposomal drug delivery system enhances mitoxantrone antitumor activity. *Nat. Biotechnol.*, **17**, 775–779.
14. Holland,J.W., Cullis,P.R. and Madden,T.D. (1996) Poly(ethylene glycol)-lipid conjugates promote bilayer formation in mixtures of non-bilayer-forming lipids. *Biochemistry*, **35**, 2610–2617.
15. Silvius,J.R. and Leventis,R. (1993) Spontaneous interbilayer transfer of phospholipids: dependence on acyl chain composition. *Biochemistry*, **32**, 13318–13326.
16. Hu,Q., Shew,C.R., Bally,M.B. and Madden,T.D. (2001) Programmable fusogenic vesicles for intracellular delivery of antisense oligodeoxynucleotides: enhanced cellular uptake and biological effects. *Biochim. Biophys. Acta*, **1514**, 1–13.
17. Hope,M.J., Bally,M.B., Webb,G. and Cullis,P.R. (1985) Production of large unilamellar vesicles by a rapid extrusion procedure: characterization of size distribution, trapped volume and ability to maintain a membrane potential. *Biochim. Biophys. Acta*, **852**, 123–126.
18. Mayer,L.D., Hope,M.J., Cullis,P.R. and Janoff,A.S. (1985) Solute distributions and trapping efficiencies observed in freeze-thawed multilamellar vesicles. *Biochim. Biophys. Acta*, **817**, 193–196.
19. Pichon,C., Monsigny,M. and Roche,A.C. (1999) Intracellular localization of oligonucleotides: influence of fixative protocols. *Antisense Nucleic Acid Drug Dev.*, **9**, 89–93.
20. Roehm,N.W., Rodgers,G.H., Hatfield,S.M. and Glasebrook,A.L. (1991) An improved colorimetric assay for cell proliferation and viability utilizing the tetrazolium salt XTT. *J. Immunol. Methods*, **142**, 257–265.
21. Chelly,J. and Kahn,A. (1994) RT-PCR and mRNA quantitation. In Mullis,K.B., Ferré,F. and Gibbs,R.A. (eds), *The Polymerase Chain Reaction*. Birkhäuser, Boston, MA, pp. 97–109.
22. Zelphati,O. and Szoka,F.C. (1996) Intracellular distribution and mechanism of delivery of oligonucleotides mediated by cationic lipids. *Pharm. Res.*, **13**, 1367–1372.
23. Marcusson,E.G., Bhat,B., Manoharan,M., Bennett,C.F. and Dean,N.M. (1998) Phosphorothioate oligodeoxynucleotides dissociate from cationic lipids before entering the nucleus. *Nucleic Acids Res.*, **26**, 2016–2023.
24. Islam,A., Handley,S.L., Thompson,K.S.J. and Akhtar,S. (2000) Studies on uptake, sub-cellular trafficking and efflux of antisense oligodeoxynucleotides in glioma cells using self-assembling cationic lipoplexes as delivery systems. *J. Drug Target.*, **7**, 373–382.
25. Shi,F., Nomden,A., Oberle,V., Engberts,J.B. and Hoekstra,D. (2001) Efficient cationic lipid-mediated delivery of antisense oligonucleotides into eukaryotic cells: down-regulation of the corticotropin-releasing factor receptor. *Nucleic Acids Res.*, **29**, 2079–2087.
26. Jansen,B., Schlagbauer-Wadl,H., Brown,B.D., Bryan,R.N., Van Elsas,A., Müller,M., Wolf,K., Eichler,H.G. and Pehamberger,H. (1998) bcl-2 antisense therapy chemosensitizes human melanoma in SCID mice. *Nature Med.*, **4**, 232–234.
27. Konopka,K., Rossi,J.J., Swideski,P., Slepushkin,V.A. and Düzgünes,N. (1998) Delivery of an anti-HIV ribozyme into HIV-infected cells via cationic liposomes. *Biochim. Biophys. Acta*, **1372**, 55–68.
28. Zamecnik,P.C. and Stephenson,M.L. (1978) Inhibition of Rous sarcoma virus replication and cell transformation by a specific oligodeoxynucleotide. *Proc. Natl Acad. Sci. USA*, **75**, 280–284.
29. Nemunaitis,J., Holmlund,J.T., Kraynak,M., Richards,D., Bruce,J., Ognoskie,N., Kwoh,T.J., Geary,R.S., Dorr,A., Von Hoff,D. and Eckhardt,S.G. (1999) Phase I evaluation of ISIS 3521, an antisense oligodeoxynucleotide to protein kinase C-alpha, in patients with advanced cancer. *J. Clin. Oncol.*, **17**, 3586–3595.
30. Yuen,A.R., Halsey,J., Fisher,G.A., Holmlund,J.T., Geary,R.S., Kwoh,T.J., Dorr,A. and Sikic,B.I. (1999) Phase I study of an antisense oligonucleotide to protein kinase C-alpha (ISIS 3521/CGP 64128A) in patients with cancer. *Clin. Cancer Res.*, **5**, 3357–3363.
31. Cunningham,C.C., Holmlund,J.T., Schiller,J.H., Geary,R.S., Kwoh,T.J., Dorr,A. and Nemunaitis,J. (2000) A phase I trial of c-Raf kinase antisense oligonucleotide ISIS 5132 administered as a continuous

intravenous infusion in patients with advanced cancer. *Clin. Cancer Res.*, **6**, 1626–1631.
32. Waters,J.S., Webb,A., Cunningham,D., Clarke,P.A., Raynaud,F., di Stefano,F. and Cotter,F.E. (2000) Phase I clinical and pharmacokinetic study of bcl-2 antisense oligonucleotide therapy in patients with non-Hodgkin's lymphoma. *J. Clin. Oncol.*, **18**, 1812–1823.
33. Loke,S.L., Stein,C.A., Zhang,X.H., Mori,K., Nakanishi,M., Subasinghe,C., Cohen,J.S. and Neckers,L.M. (1989) Characterization of oligonucleotide transport into living cells. *Proc. Natl Acad. Sci. USA*, **86**, 3474–3478.
34. Yakubov,L.A., Deeva,E.A., Zarytova,V.F., Ivanova,E.M., Ryte,A.S., Yurchenko,L.V. and Vlassov,V.V. (1989) Mechanism of oligonucleotide uptake by cells: involvement of specific receptors? *Proc. Natl Acad. Sci. USA*, **86**, 6454–6458.
35. Beltinger,C., Saragovi,H.U., Smith,R.M., LeSauteur,L., Shah,N., DeDionisio,L., Christensen,L., Raible,A., Jarett,L. and Gewirtz,A.M. (1995) Binding, uptake and intracellular trafficking of phosphorothioate-modified oligodeoxynucleotides. *J. Clin. Invest.*, **95**, 1814–1823.
36. Silvius,J.R. and Zuckermann,M.J. (1993) Interbilayer transfer of phospholipid-anchored macromolecules via monomer diffusion. *Biochemistry*, **32**, 3153–3161.
37. Zelphati,O. and Szoka,F.C. (1996) Mechanism of oligonucleotide release from cationic liposomes. *Proc. Natl Acad. Sci. USA*, **93**, 11493–11498.
38. Noguchi,A., Furuno,T., Kawaura,C. and Nakanishi,M. (1998) Membrane fusion plays an important role in gene transfection mediated by cationic liposomes. *FEBS Lett.*, **433**, 169–173.
39. Fisher,T.L., Terhorst,T., Cao,X.D. and Wagner,R.W. (1993) Intracellular disposition and metabolism of fluorescently labeled unmodified and modified oligonucleotides microinjected into mammalian cells. *Nucleic Acids Res.*, **21**, 3857–3865.
40. Shew,C.R. (2001) Characterization of liposomal drug delivery systems utilizing cell culture methods. PhD thesis, University of British Columbia.
41. Miller,C.R., Bondurant,B., McLean,S.D., McGovern,K.A. and O'Brien,D.F. (1998) Liposome-cell interactions *in vitro*: effect of liposome surface charge on the binding and endocytosis of conventional and sterically stabilized liposomes. *Biochemistry*, **37**, 12875–12883.
42. Mui,B., Ahkong,Q.F., Chow,L. and Hope,M.J. (2000) Membrane perturbation and the mechanism of lipid-mediated transfer of DNA into cells. *Biochim. Biophys. Acta*, **1467**, 281–292.
43. Fattal,E., Nir,S., Parente,R.A. and Szoka,F.C. (1994) Pore-forming peptides induce rapid phospholipid flip-flop in membranes. *Biochemistry*, **33**, 6721–6731.
44. Veal,G.J., Agrawal,R.A. and Byrn,R.A. (1998) Sequence-specific RNase H cleavage of *gag* mRNA from HIV-1 infected cells by an antisense oligonucleotide *in vitro*. *Nucleic Acids Res.*, **26**, 5670–5675.
45. Sawai,Y., Kitahara,N., Thung,W.L., Yanokura,M. and Tsukada,K. (1981) Nuclear location of ribonuclease H and increased level of magnesium-dependent ribonuclease H in rat liver on thioacetamide treatment. *J. Biochem.*, **90**, 11–16.